Received: March 21, 2024. Revised: April 19, 2024.

INASS

International Journal of
Intelligent Engineering & Systems

http://www.inass.org/

Design and Analysis of Grouping Non-Active Frequency -Time Index Modulation for Differential Chaos Shift Keying Communication System

Ruaa Abdulkareem Yaseen[1]* **Fadhil S. Hasan[1]**

[1]*Department of Electrical Engineering, Al-Musansiriyah University, Iraq*
* Corresponding author's Email: ruaa.k.yaseen@uomustansiriyah.edu.iq

Abstract: This paper introduces a new index modulation method called Grouping Frequency-Time Index Modulation Non-Active for Differential Chaos Shift Keying (GFTIM-DCSK-II). The proposed system exploits the advantages of index modulation (IM) so that both the energy and spectrum efficiency of the system are enhanced. The suggested system effectively employs both frequency and time resources, allowing for efficient transmission at large data rates. For each symbol period, the new approach divides all data bits into equal G groups. For each group, the system includes frequency index bits, denoted as m_1, which are utilized to choose a non-active subcarrier from a total of 2^{m_1} subcarriers. Additionally, time index bits, denoted as m_2, are employed to select a single time slot from 2^{m_2} total time slots. After that, the modulated bits m_0 are subjected to DCSK modulation and thereafter sent over the active subcarriers. Therefore, $G(m_0+m_1+m_2)$, where $m_0 = (2^{m_1}2^{m_2} - 1)$, is the total amount of bits transmitted with the GFTIM-DCSK-II system. To better demonstrate the distinctive characteristics of the proposed scheme the energy efficiency, complexity, and spectral efficiency of the GFTIM-DCSK-II system in comparison to the most advanced alternatives available are thoroughly analyzed. The system with q=8, m_1=1, and m_2=1 saves around 40% more energy than the CTIM-DCSK system also the proposed system enhanced the spectral efficiency around five times more than CTIM-DCSK and GSIMDCSK-II with q=8, m_1=1, and m_2=4. Bit error rate (BER) formulas across multipath Rayleigh fading channels and additive white Gaussian noise (AWGN) are calculated analytically. The proposed system showed an enhancement in BER performance around 5 dB than CI-DCSK2 and GSTIM-DCSKII across the AWGN channel at a BER of 10^{-4} at the same data rate.

Keywords: Frequency-Time index modulation, Spectral efficiency, DCSK, Energy efficiency, Multipath Rayleigh fading channels.

1. Introduction

Over the past 20 years, the use of chaotic signals in spread spectrum communication systems has grown in popularity. The primary cause is the broad spectrum, impulse-like auto-correlation, low cross-correlation values, and ease of generation of such signals [1]. These features are crucial for enhancing multiple access performance, increasing resilience to jamming or interference, and improving tolerance against multipath effects. In addition, the non-periodic aspect of the transmission enhances its security when employed coherently.

In general, chaotic communication may be classified into coherent and noncoherent methods based on whether the receiver requires perfect reproductions of the unmodulated chaotic carriers [1]. A chaotic shift keying (CSK) system with a coherent receiver is described in [2] as a type of coherent modulation. Nevertheless, achieving complete chaotic synchronization remains challenging inside the CSK scheme. Nevertheless, achieving complete chaotic synchronization remains challenging inside the CSK scheme. Conversely, non-coherent chaotic modulation techniques, such as differential chaos shift keying (DCSK), have garnered significant interest due to their ability to recover the signal at the reception side without requiring synchronization or channel information estimation [3,4]. As non-information-carrying reference samples are sent for half of the bit period

[1], DCSK's data rate and energy efficiency are extremely low.

Various modifications to DCSK techniques have been suggested to improve energy efficiency or data throughput. A quadrature chaos-shift keying (QCSK) is introduced in [5] as a method to increase the data rate of traditional DCSK while maintaining the same frame duration. In [6], a high-efficiency DCSK (HE-DCSK) is presented. By recycling each reference slot and allowing two bits of data to be conveyed in a single data-modulated sample sequence, this technique doubles the information rate. Additionally, by reducing retransmissions, this doubles bandwidth efficiency and reduces the possibility of interception of the sent signal. However, compared to DCSK, the system's complexity rises.

To decrease the level of noise variation experienced by the receiver, a noise-reduction differential chaos shift keying (NR-DCSK) technique is suggested in reference [7]. A short reference DCSK (SR-DCSK) system is suggested in [8], where reference signals are abbreviated to reduce their duration. To raise data throughput and enhance energy efficiency without lowering the performance of BER. The authors in [9] have proposed an improved DCSK (I-DCSK) to decrease the duration of transmission per bit and improve the information rate.

A novel approach called multi-carrier DCSK (MC-DCSK) has been suggested as a means to accomplish fast transmission of large amounts of data [10]. This technique is an expansion of DCSK modulation that operates in parallel by utilizing several subcarriers to deliver the whole signal. This configuration eliminates the need for a radio frequency (RF) delay circuit in the transceiver.

The next generation of wireless communications systems is actively investigating important ways to deliver high-data-rate communication services in response to the increasing need for higher-data-rate communications brought on by the continuous development of smart devices and smartphone applications [11]. Index modulation (IM) has gained significant attention in recent years as a competitive approach for 5G wireless communications systems [12]. IM has been acknowledged as an innovative method to meet the need for high data information rate transmission. Within the IM setup, just a portion of specific indexed entities, such as antennas, spreading codes, subcarriers, and time slots, are utilized for transmitting information, while the remaining entities remain inactive [13]. During this operation, extra data bits are conveyed implicitly through the index symbols. In the context of a communication network that requires low complexity and low energy consumption, a method called frequency index modulation is suggested in reference [14]. This method involves using a simple square-law envelope detector to determine the active frequency index, which allows for the recovery of the indexed bits.

According to the benefits of IM, the IM concept was used on DCSK-based structures, like CS-DCSK and OM-DCSK, and to achieve greater data rates, two types of code index modulation aided DCSK systems called CIM-CS-DCSK [15] and CIM-OM-MDCSK [16], respectively were created. In a recent publication [17], a novel non-coherent commutation code index called CCI-DCSK, was introduced. The CCI-DCSK method utilizes the advantages of IM by assigning additional bits to separate replicated versions of the reference chaotic sequence. These replicated sequences are then employed to distribute a modulated bit. In references [18] and [19], the authors introduce an innovative IM approach specifically designed for spread spectrum (SS) systems. This technique, known as code index modulation (CIM), maps extra data into the indices of various codes which are utilized to distribute modulated bits to improve the data rate.

Additionally, the IM was added to the multicarrier DCSK (MC-DCSK) system [20], allowing the data rate of the MC-DCSK system to be improved. This was made possible by the proposed carrier index differential chaos shift keying (CI-DCSK) [21], generalized CI-DCSK system (GCI-DCSK) [22], and the M-ary CI-DCSK system (CI-MDCSK) [23]. Under the CI-DCSK scheme, the activation of subcarriers is limited, leading to an inefficient utilization of spectrum resources.

A two-layer CI-DCSK (2CI-DCSK) has been proposed in [24] to enhance the recycling of subcarrier resources and achieve improved spectral efficiency and energy efficiency in CI-DCSK. A dual-index-modulation-aided DCSK technique (DCSK-DIM) was proposed in [25]. Enhancing the data information rate of the suggested system, the DCSK-DIM system may repurpose all available time slots for transmitting extra data bits. In contrast to the utilization of many subcarriers, the utilization of a single carrier introduces a constraint to the system, alongside other limitations associated with the implementation of a substantial spread factor length and a significant quantity of delay units.

In [26], a novel approach called Joint Code-Frequency with Index Modulation (CFIM) is suggested. CFIM combines two forms of index modulation, one based on code and the other on frequency. The input information bits are split into equal blocks of K in this system. Each sub-block

further separates its bits into three components; one part is mapped as a carrier index, the second part is mapped as a code index, and the third part describes the actual bits that are transmitted through M-ary modulation. To mitigate the multipath effect, it is necessary to have knowledge of the channel status, equalization, and synchronization. These requirements are seen as drawbacks of the system.

To improve transmission reliability while minimizing complexity, a method based on index-modulation-aided DCSK called CTIM-DCSK is proposed in [27]. Both frequency and time resources are utilized by this system. The proposed approach enables the transfer of extra information bits by utilizing the resources of both the time and carrier indices. In this system, a noise reduction operation is used at the receiver to improve the BER performance. This system has a higher complexity.

The GSIM-DCSKI and GSIM-DCSKII schemes are two recommended variations of the grouping subcarrier with index modulation-based DCSK that may be present in [28]. Higher data rates and energy efficiency are offered by these schemes compared to conventional CI-DCSK systems.

In [29], two new GSIM-DCSK with permutation index modulation (PI) systems, GSPIM-DCSKI and GSPIM-DCSKII, are introduced. These schemes aim to improve energy, data rate, and spectral efficiency. In this system, the length of the chaotic signal (spreading factor) is large to ensure the semi-orthogonal of the basis. Therefore, a longer duration is needed. Also, these systems demonstrate greater complexity due to the increased amount of multiplication operations and the employment of permutation blocks in both the transmission and receiving sides.

In this study, the suggested technique, called grouping non-active frequency-time index modulation (GFTIM-DCSK-II), utilizes both frequency and time resources as index entities, while in the GSIM-DCSK system [28] and the CI-DCSK system [21] the frequency resource is only utilized as the index entity. Hence, with this system, it is feasible to send extra information bits by utilizing the existing frequency and time index resources. Furthermore, the suggested system employs orthogonal sinusoidal carriers for the transmission of both the reference-chaotic and information-bearing signals. The contributions to this work are outlined as follows:

1. A grouping frequency-time index modulation GFTIM-DCSK-II is proposed. The information bits in this system are separated into G groups of equal size. The data information bits within each sub-block consist of three components: the modulated bits, frequency index bits, and time index bits. In the GFTIM-DCSK-II system, the chosen subcarriers utilize time slots that transmit identical index bits. Within each sub-group, m_1 bits are utilized to assign symbols to designate a single non-active subcarrier out of a total of 2^{m_1} subcarriers. Similarly, m_2 bits are used to assign symbols to pick one out of 2^{m_2} time slots. On the other hand, the modulated bits $m_0 = (2^{m_1} 2^{m_2} - 1)$ are first sent via the active subcarriers and then modulated using the DCSK approach. Consequently, the number of bits carried increases to $G(m_0 + m_1 + m_2)$ bits for each symbol duration.
2. To further demonstrate the advantages of our design, we compare the GFTIM-DCSK-II system to the CI-DCSK2, GSIM-DCSKII, and CTIM-DCSK systems in terms of data rate, complexity, energy efficiency, and spectral efficiency.
3. The analytical bit error rate (BER) formulas for both the additive white Gaussian noise (AWGN) channel and the multipath Rayleigh fading channel are derived.

The remaining content of the paper can be outlined as follows. Section 2 introduces the suggested GFTIM-DCSK-II system model. Energy efficiency, spectral efficiency, and complexity are analyzed in section 3. The analytical BER of GFTIM-DCSK-II is demonstrated in Section 4. Numerical and simulation results are discussed in Section 5, and concluding observations are provided in Section 6.

2. Proposed GFTIM-DCSK-II system model

Fig. 1 shows the transmitter for the suggested system. In the suggested system, we use a second-order Chebyshev polynomial function (i.e., $x_{q,k+1} = 1 - 2x_{q,k}^2$ where $k = 1, 2, \ldots$) to create a reference chaotic signal with length R, $x_k = [x_1, x_2, \ldots, x_R]$. During the r^{th} symbol period, the chaotic sequence generated by the chaotic generator is inputted into the pulse shaping filter depicted in Fig. 1. The resulting chaotic signal is then delivered as a current reference signal through the reference subcarrier, with a central frequency denoted as f_0.

$$x_r(t) = \sum_{k=1}^{R} x_{r,k}\, h(t - kT_c) \tag{1}$$

where T_c and $h(t)$ represent the chip time and the square-root-raised cosine filter, respectively.

In the GFTIM-DCSK-II transmitter, the input bit stream in each r^{th} symbol duration is divided into G blocks of equal size, where each block consists of $m = (m_0 + m_1 + m_2)$ bits. Thus,

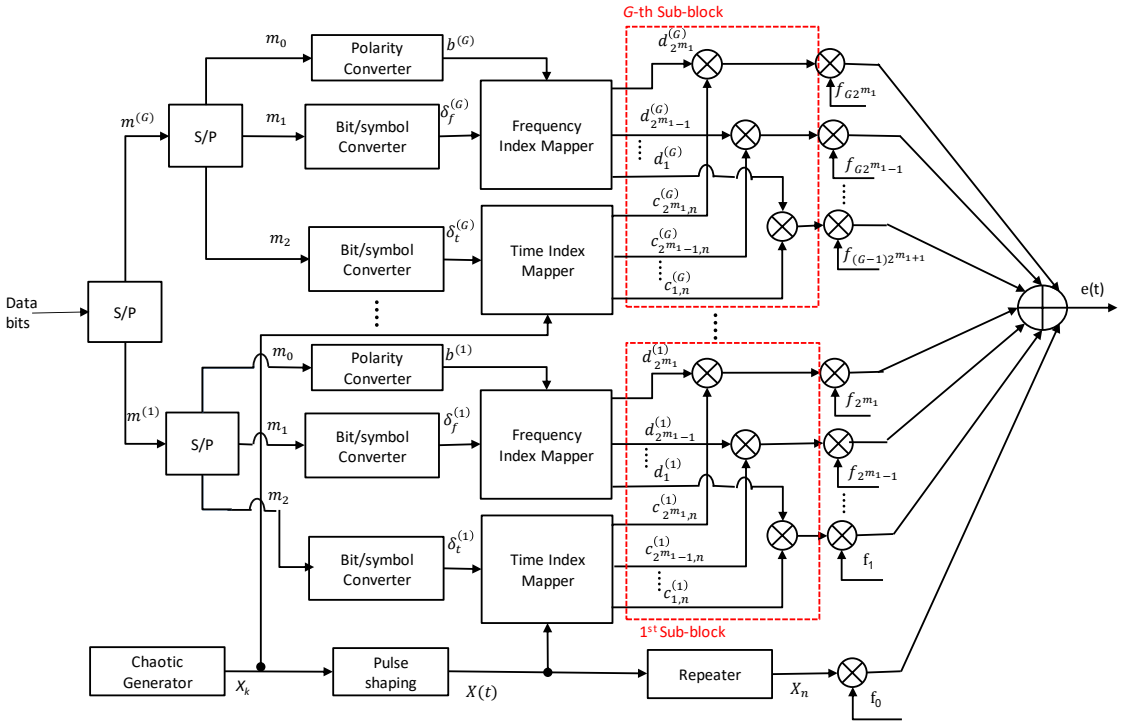

Figure. 1 Transmitter structure of GFTIM-DCSK-II scheme

$G(m_0 + m_1 + m_2)$ is the total number of bits conveyed in each r^{th} symbol period. With this format, m_0= ($2^{m_1}2^{m_2}$ -1) represents the number of modulated bits that are sent within every sub-block. Furthermore, $\log_2 N_f = m_1$ is the number of frequency-mapped bits needed for selecting one non-active subcarrier among $2^{m_1} = N_f$ subcarriers, and $\log_2 N_t = m_2$ is the number of mapped bits needed to select a single time slot among $2^{m_2} = N_t$ time slots. There are $(2^q + 1)$ subcarriers in total, where q is an integer value and $m_1 \leq q$. Of these, one conveys the reference chaotic signal. The rest of the subcarriers are organized into G sets, whereby each set consists of N_f subcarriers; that is, $G = 2^{q-m_1}$. There are $(N_f - 1)$ active subcarriers and one non-active subcarrier in each sub-block, determined by the frequency-time mapped bits.

In the g^{th} sub-block, each modulated bit is transformed to $b_r = \{1, -1\}$ using the polarity converter. By using DCSK modulation, information bits are carried by each active subcarrier. Consider two position index modulation symbols, δ_f and δ_t, which are defined by the frequency index bits and the time index bits, respectively. For every sub-block, the m_1 and m_2 indexed bits are transformed into index symbols δ_f and δ_t, respectively.

One time slot and one subcarrier are selected in a particular sub-block, resulting in the formation of sequences denoted as $d^g_{r,i,j}$, where $g = 1, \ldots, G$ and $1 \leq i < N_f, 1 \leq j \leq N_t$. When $i \neq \delta_f$ and $j \neq \delta_t$, the value of $d^g_{r,i,j}$, which can have values of either +1 or −1, is determined by the g^{th} modulated bits (b^g). If not, equals zero. After that, the reference-chaotic signal $x_r(t)$ is multiplied by $d^g_{r,i,j}$ to convey the information bits.

Consequently, $\beta = N_t R$, where R is the duration of a reference-chaotic signal, is the spreading factor of the GFTIM-DCSK-II system. Ultimately, the reference-chaotic signal $x_n(t)$ and the information-bearing signals are sent via the subcarrier at frequency f_i.

Table 1 displays a basic mapping rule for the values of $q = 2$, $m_1 = 1$, and $m_2 = 1$. There are $G = 2$ sub-blocks, and each sub-block has four coefficients: $d^g_{(i,j)} \in Z^g$, $Z^g \in \mathbb{R}^{N_f \times N_t}$, $i = 1,2$, $j = 1,2$, $g = 1,2$. Additionally, each sub-block's active frequencies and time slots are displayed in this table. For example, sub-blocks 1 and 2 use the patterns f_1 f_2 t_1 t_2 and f_3 f_4 t_1 t_2, respectively.

Therefore, the signal transmitted in the r^{th} frame is expressed as

$$e(t) = \sum_{g=1}^{G} \sum_{i=1}^{N_f} b^g \, c^g_{i,n} \, cos\left(2\pi f_{(g-1)N_f+i} t + \phi_{(g-1)N_f+i}\right) + x_r(t) cos(2\pi f_0 t + \phi_0) \quad (2)$$

$$c_{i,n} = \left[c_{i,1,k}, c_{i,2,k}, \ldots, c_{i,N_t,k}\right] \quad (3)$$

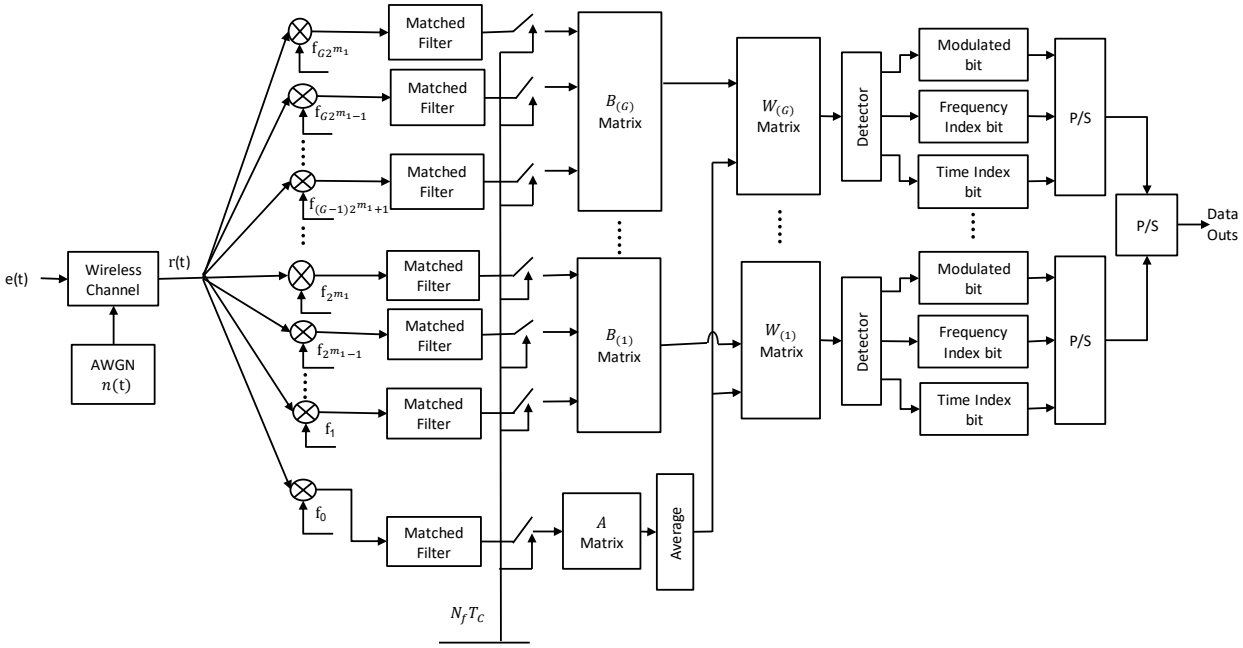

Figure. 2 Receiver structure of GFTIM-DCSK-II scheme

$$c_{i,j,k} = \begin{cases} x_k & j \neq \delta_t \\ 0 & otherewise \end{cases} \quad (4)$$

The variables $f_{(g-1)N_f+i}$ and $\phi_{(g-1)N_f+i}$ denote the center frequency and phase angle, respectively, of the i^{th} subcarrier in the g^{th} sub-block.

At the receiver side in Fig. 2, given the assumption that multipath fading and AWGN have tainted the sent signal $e(t)$, the received signal $r(t)$ may be expressed as

$$r(t) = \sum_{l=1}^{P} \alpha_l \delta(t - \tau_l) \otimes e(t) + n(t) \quad (5)$$

The symbol ⊗ denotes the operation of convolution, and $n(t)$ is the AWGN with a zero mean and a variance of N_0 /2. In this research, the channel coefficients α_l are considered to be Rayleigh distribution independent random variables. Firstly, the orthogonally modulated carrier frequencies corresponding to N_f + 1 are used to separate the incoming signal.

Every $N_f T_c$ instant, the signals are sampled after being filtered by the matching filters. The discrete signals that have been demodulated are then recorded into two matrices. A matrix A of dimension $1 \times \beta$, where β is specified as $\beta = N_t R$, is used to represent the reference chaotic signals. The second matrix is B^g of dimensions $R \times (N_f N_t)$, where G varies from 1 to g, representing the information-bearing signals of the g^{th} sub-block.

$$B^g = [B_1\ B_2\ B_3, \dots, B_N],\ B_i \in \mathbb{R}^{R \times N_f} \quad (6)$$

Where

$$B_i = \begin{bmatrix} d_i\, c_{i,1,1} & d_i\, c_{i,2,1}\ , \dots, d_i\, c_{i,N_t,1} \\ d_i\, c_{i,1,2} & d_i\, c_{i,2,2}\ , \dots, d_i\, c_{i,N_t,2} \\ & \vdots \\ d_i\, c_{i,1,R} & d_i\, c_{i,2,1}\ , \dots, d_i\, c_{i,N_t,R} \end{bmatrix},\ 1 \leq i \leq N_f \quad (7)$$

The received reference-chaotic signals are subjected to an average and summation operation. The signal that results from averaging the reference-chaotic signal is then used to demodulate the signals that convey the information. Consequently, the average reference chaotic signal is shown as

$$\tilde{x}_{avg,k} = \frac{1}{N_t} \sum_{j=1}^{N_t} \sum_{l=1}^{P} \alpha_l\, x_{j,k-\tau_l} + n_j^k \quad (8)$$

$$\tilde{n}_k = \frac{1}{N_t} \sum_{j=1}^{N_t} n_j^k \quad (9)$$

Following this, the correlation matrices W_r^g for the r^{th} symbol and g^{th} group where $1 \leq g \leq G$, and each matrix has a $1 \times (NQ)$ dimension are computed as

$$W_r^g = \tilde{x}_{avg,k}{}^T \times\ B^g = \left[W_{r,1}^g\ W_{r,2}^g \dots\ W_{r,2^{m_1+m_2}}^g\right]^T \quad (10)$$

Table 1. Mapping rule for the first sub-block (g =1), q=2, m_1=1, m_2 =1, (* f_i selected frequency for the g^{th} sub-block, t_j selected time for the g^{th} sub-block)

Modulated bit	**Polarity converter**	**Frequency index bit**	**Time index bit**	**Index of non-active subcarrier** $(\boldsymbol{\delta_f}, \boldsymbol{\delta_t})_r^g$	$\boldsymbol{Z^g}$	$(\boldsymbol{f_i}, \boldsymbol{t_j})$*
0	-1	0	0	1,1	$\begin{bmatrix} 0 & -1 \\ -1 & -1 \end{bmatrix}$	(f_1, t_1)
0	-1	0	1	1,2	$\begin{bmatrix} -1 & 0 \\ -1 & -1 \end{bmatrix}$	(f_1, t_2)
0	-1	1	0	2,1	$\begin{bmatrix} -1 & -1 \\ 0 & -1 \end{bmatrix}$	(f_2, t_1)
0	-1	1	1	2,2	$\begin{bmatrix} -1 & -1 \\ -1 & 0 \end{bmatrix}$	(f_2, t_2)
1	1	0	0	1,1	$\begin{bmatrix} 0 & 1 \\ 1 & 1 \end{bmatrix}$	(f_1, t_1)
1	1	0	1	1,2	$\begin{bmatrix} 1 & 0 \\ 1 & 1 \end{bmatrix}$	(f_1, t_2)
1	1	1	0	2,1	$\begin{bmatrix} 1 & 1 \\ 0 & 1 \end{bmatrix}$	(f_2, t_1)
1	1	1	1	2,2	$\begin{bmatrix} 1 & 1 \\ 1 & 0 \end{bmatrix}$	(f_2, t_2)

The minimum absolute of $W_{r,\zeta}^g$ for ζ ranging from 1 to $2^{m_1+m_2}$ is used to calculate the frequency and time index bits within the g^{th} sub-block to identify the non-active subcarrier. This value may be expressed as:

$$(\widetilde{\delta_f}, \widetilde{\delta_t})_r^g = \arg \min_{\substack{i=1,..,N_f \\ j=1,..,N_t}} \left(\left|W_r^g(i,j)\right|\right),\ g = 1,..,G \tag{11}$$

$(\widetilde{\delta_f}, \widetilde{\delta_t})_r^g$ denotes the non-active subcarrier's estimated frequency and time index in the g^{th} sub-block. The index bits predicted for the g^{th} sub-block are determined by translating $(\widetilde{\delta_f}, \widetilde{\delta_t})_r^g$ into a binary number using Table 1 in reverse mapping. By detecting the indices of frequency and time slots, we may estimate the modulated bits, $\hat{a}_b$ as:

$$\hat{a}_b = \begin{cases} 0 & if\ sign\left(W_{r,i,j}^g\right) < 0 \\ 1 & otherwise \end{cases},\ g = 1,..,G \tag{12}$$

Where $b = 1,\ldots,m_0$, $i \neq \widetilde{\delta_f}$ and $j \neq \widetilde{\delta_t}$.

3. System analysis

3.1 Energy efficiency and spectral efficiency

The proposed GFTIM-DCSK-II modulates just Gm_0 bits of the total $G(m_0 + m_1 + m_2)$ directly by DCSK modulation, whereas $G(m_1 + m_2)$ bits are conveyed through subcarrier selection. Given that each modulated bit has to be sent with an energy of E_b, the mapping between index subcarriers and time slots should decrease the overall energy needed for transmission. Thus, in the suggested GFTIM-DCSK-II, the percentage of energy savings is provided by [26]:

$$E_{saving} = \left(1 - \frac{m_0}{(m_0 + m_1 + m_2)}\right) E_b\% = \left(1 - \frac{1}{\left(1 + {}^{m_1}/_{m_0} + {}^{m_2}/_{m_0}\right)}\right) E_b\% \tag{13}$$

Given that $m_1 = \log_2 N_f$ and $m_2 = \log_2 N_t$ have been specified, the energy savings are determined by the ratio of the number of subcarriers

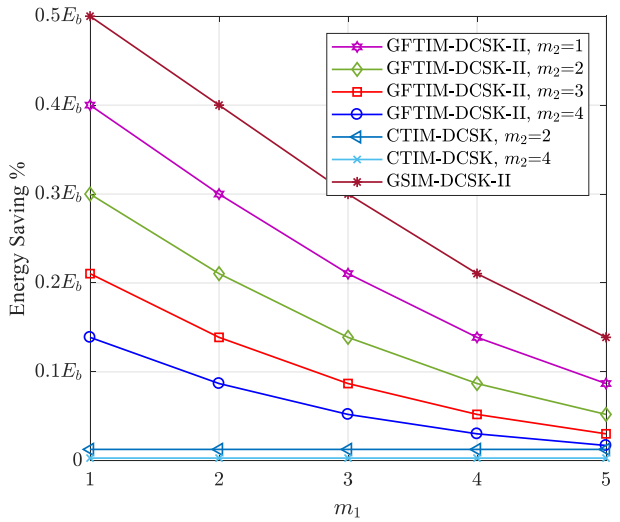

Figure. 3 Comparisons of Energy Saving versus m_1 values for GFTIM-DCSKII with different DCSK techniques at q=8

Table 2. Energy saving

Modulation	Energy saving
CI-DCSK2 [21]	$\left(1-\frac{(2^q-1)}{(q+2^q-1)}\right)E_b\%$
GSIM-DCSK-II [28]	$\left(1-\frac{(2^{m_1}-1)}{m_1+(2^{m_1}-1)}\right)E_b\%$
CTIM-DCSK [27]	$\left(1-\frac{(2^q-1)(2^{m_2}-1)}{m_1+m_2+(2^q-1)(2^{m_2}-1)}\right)E_b\%$
GFTIM-DCSK-II	$\left(1-\frac{m_0}{m_0+m_1+m_2}\right)E_b\%$

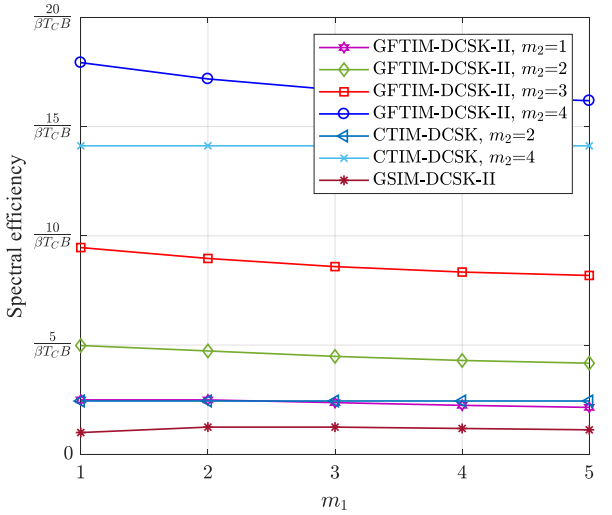

Figure. 4 Comparisons of Spectral efficiency versus m_1 values for GFTIM-DCSKII with different DCSK techniques at q=8

and time slots used for indexing to the system's modulation order. As seen in Fig. 3, Observed that an increase in the number of time slots or a decrease in the number of subcarriers to be indexed results in additional energy savings in the GFTIM-DCSK-II system for a fixed modulation order. Table 2 presents a comparative analysis of energy savings across various DCSK modulations.

Table 3. Spectral efficiency

Modulation	Spectral efficiency
CI-DCSK2 [21]	$\frac{M-1+q}{(M+1)\,\beta T_c B}$
GSIM-DCSK-II [28]	$\frac{M(m_1+2^{m_1}-1)}{(N_f\,(M+1)\,\beta T_c B}$
CTIM-DCSK [27]	$\frac{N_t(q+m_2+(M-1)(N_t-1))}{(N_t+1)M\beta T_c B}$
GFTIM-DCSK-II	$\frac{M(m_0+m_1+m_2)}{N_f\,(M+1)\,\beta T_c B}$

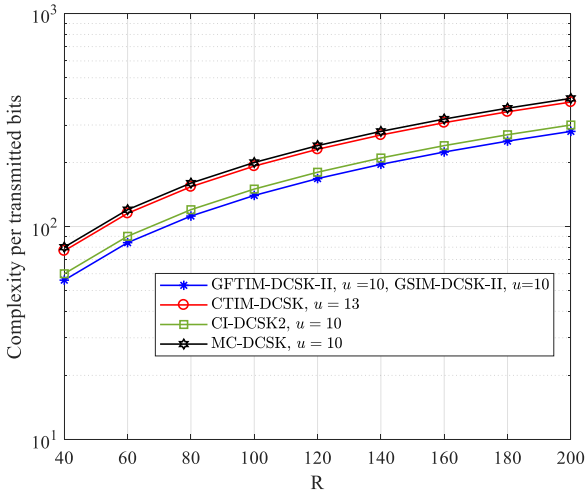

Figure. 5 Comparisons of Complexity per transmitted bit versus R values for GFTIM-DCSKII with different DCSK techniques at q=8

Table 4. System complexity

Modulation	Complexity per transmitted bits
MC-DCSK	$\frac{2MR}{M}$
CI-DCSK2	$\frac{(M-1)R+MR}{M-1+\log_2 M}$
GSIM-DCSK-II	$\frac{G[(N_f-1)R+N_fR]}{G(N_f-1+\log_2 N_f)}$
CTIM-DCSK	$\frac{[(M-1)(N_t-1)]R+MN_tR}{(M-1)(N_t-1)+\log_2 M+\log_2 N_t}$
GFTIM-DCSK-II	$\frac{G[(N_fN_t-1)R+N_fN_tR]}{G(m_0+m_1+m_2)}$

Spectral efficiency is an essential factor for evaluating the system's performance. The spectral

efficiency is determined in this research using the bit rate to total bandwidth ratio. The spectral efficiency of the proposed system can be expressed as follows:

$$\Psi_{GFTIM-DCSK} = \frac{bit\ rate}{total\ bandwidth} = \frac{\frac{G(m_0+m_1+m_2)}{\beta T_c}}{(2^q+1)B} = \frac{G(m_0+m_1+m_2)}{(2^q+1)\beta T_c B} \quad (14)$$

Considering that each subcarrier has the same bandwidth and is represented by B. Fig. 4 shows the spectral efficiency of several DCSK communication systems as well as the suggested GFTIM-DCSK-II system. A comparative analysis of the spectral efficiencies of several DCSK techniques is shown in Table 3. The spectral efficiency of the GFTIM-DCSK-II system is represented by the variables M and m_1, where $G = M/2^{m_1}$, $M = 2^q$.

3.2 System complexity

This subsection evaluates and compares the complexity of the GFTIM-DCSK-II system with other chaotic communication systems such as MC-DCSK, CI-DCSK2, CTIM-DCSK, and GSIM-DCSK-II. The total number of multiplication operations that take place at the side of the transmitter and receiver are the basis for the complexity study. Hence, the complexity of the GFTIM-DCSK-II system may be computed as $O_{GFTIM\_DCSK\_II} = G[(N_f N_t - 1)R + N_f N_t R]$. Table 4 illustrates the complexity of several DCSK systems.

Fig. 5, shows the complexity of each transmitted bit for various DCSK systems vs the spreading factor R. The number of transmitted bits per symbol is shown by u. The parameter values for GFTIM-DCSK=II, MC-DCSK, CI-DCSK2, CTIM-DCSK, and GSIM-DCSK-II techniques are $M/N_f/N_t$= 4/2/2, M = 10, M = 8, M/N_t = 4/4, and M/N_f = 8/4. From this Figure, it is seen that the system complexity of the mentioned techniques rises proportionally with the increment of R. The GFTIM-DCSK-II system has lower system complexity than the other comparable systems.

4. BER performance analysis

To simplify the analysis, we assume that the highest delay caused by multipath is significantly less than the spreading factor. In other words, the maximum delay (τ_{max}) is much smaller than the spreading factor $0 < \tau_{max} \ll R$. Therefore, this study does not have consideration for inter-symbol interference (ISI) [21], [28], [30]. In addition, the channel is assumed to be slowly Rayleigh fading, and its coefficients remain unchanged during a single symbol's period. The GFTIM-DCSK-II system has a single non-active subcarrier within each sub-block, whereas the formula (2^{m_1}-1) determines the number of active subcarriers. The total bits transmitted for all sub-blocks are $G(m_0 + m_1 + m_2)$. At the r^{th} symbol duration, the decision variables for the i^{th} active subcarrier are $W^g_{r,i,j}$, $1 \le g \le G, 1 < i \le N_f$, $1 < j \le N_t$, where $i \ne \delta_f, j \ne \delta_t$, while for the non-active subcarrier at the output of correlator are $W^g_{r,\delta_f,\delta_t}$, $1 \le g \le G$. In this case, all that is being received is noise as no data is being delivered over the non-active subcarrier. Thus, if $i = \delta_f$, and $j = \delta_t$, the component of matrix W may be expressed as:

$$W^g_{r,\delta_f,\delta_t} = \sum_{k=1}^{R}\left(\sum_{l=1}^{P} \alpha_l x_{r,k} + \widetilde{n_k}\right) * n^k_{r,i,j} \quad g = 0,1,\dots,G \quad (15)$$

For $i \ne \delta_f$ and $j \ne \delta_t$, the matrix W component becomes

$$W^g_{r,i,j} = \sum_{k=1}^{R}\left(\sum_{l=1}^{P} \alpha_l x_k d^g_{r,i,j} + \widetilde{n_k}\right) * \left(\sum_{l}^{P} \alpha_l x_k + n^k_{i,j}\right), \quad g = 0,1,\dots,G \quad (16)$$

The variables $n^{(k)}_{r,\delta_f,\delta_t}, n^{(k)}_{r,i,j}$ and $\tilde{n}_{r,k}$ represent independent Gaussian noise components with zero mean. $\tilde{n}_{r,k}$ corresponds to the reference subcarrier, $n^{(k)}_{r,i,j}$ corresponds to the active subcarrier, and $n^{(k)}_{r,\delta_f,\delta_t}$ corresponds to the r^{th} non-active subcarrier. These components exhibit identical variances and power spectral density (PSD) of $N_0/2$. When the spreading factor R is a large value, the following approximation equation is applied [21], [24]:

$$\sum_{k=1}^{R} x_{k-\tau_l} x_{k-\tau_v} \approx 0, \quad l \ne v \quad (17)$$

To simplify the analysis, only the first sub-block is examined, as other sub-blocks in this system are comparable and follow the same operational processes. The means denoted as $E(W_{r,i,j})$, and variances denoted as $V(W_{r,i,j})$ of $W_{r,i,j}$ may be represented as:

$$E(W_{r,i,j}) = \begin{cases} 0, & i = \delta_f \text{ and } j = \delta_t \\ \sum_{l=1}^{P} \alpha^2_{r,l} \sum_{k=1}^{R} x^2_{r,k}\, d^1_{r,i,j}, & i \ne \delta_f \text{and } j \ne \delta_t \end{cases} \quad (18)$$

$$V(W_{r,i,j}) = \begin{cases} \sum_{l=1}^{P} \alpha_{r,l}^2 \sum_{k=1}^{R} x_{r,k}^2 \frac{N_0}{2} + \sum_{l=1}^{P} \alpha_{r,l}^2 \sum_{k=1}^{R} x_{r,k}^2 \\ \qquad \frac{N_0}{2N_t} + \frac{RN_0^2}{4N_t}, \ i \neq \delta_f \text{and} \ j \neq \delta_t \\ \frac{1}{2}\sum_{l=1}^{P} \alpha_{r,l}^2 \sum_{k=1}^{R} x_{r,k}^2 N_0 + \frac{RN_0^2}{4N_t}, \\ 1 < i \leq N_f, 1 < j \leq N_t \ \ where \ i = \delta_f \text{and} \ j = \delta_t \end{cases} \quad (19)$$

Within the GFTIM-DCSK-II, $E_b = \frac{(Gm_0+N_t)\sum_{k=1}^{R} x_{r,k}^2}{G(m_0+m_1+m_2)}$, where E_b represents the transmitted energy per bit, and $\gamma_b = \frac{E_b \sum_{l}^{P} \alpha_{r,l}^2}{N_0}$ The bit-to-noise ratio, or E_b/N_0. To simplify Eqs. (17) and (18) in terms of γ_b, they may be expressed as follows:

$$E(W_{r,i,j}) = \begin{cases} N_0\gamma_0\,\gamma_b = \mu_1, & i \neq \delta_f \text{and} \ j \neq \delta_t \\ 0 = \mu_2, & 1 < i \leq N_f, 1 < j \leq N_t, \\ & \text{where} \ i = \delta_f \ \text{and} \ j = \delta_t \end{cases} \quad (20)$$

$$V(W_{r,i,j}) = \begin{cases} \frac{N_0^2}{2}\left(\gamma_0\gamma_b + \frac{\gamma_0\,\gamma_b}{N_t} + \frac{R}{2N_t}\right) = \sigma_1^2, \ i \neq \delta_f \text{and} \ j \neq \delta_t \\ \frac{N_0^2}{2}\left(\gamma_0\gamma_b + \frac{R}{2N_t}\right) = \sigma_2^2, \\ 1 < i \leq N_f, 1 < j \leq N_t \ \ where \ i = \delta_f \text{and} \ j = \delta_t \end{cases} \quad (21)$$

Where $\gamma_0 = \frac{G(m_0+m_1+m_2)}{(Gm_0+N_t)}$. The BER theory of GFTIM-DCSK-II, specifically the P_{BER}, is determined by the BER of the index bits (P_{index}) and the BER of the modulated bits (P_{mod}). It may be mathematically represented as:

$$P_{BER} = \frac{m_0}{m_0+m_1+m_2} P_{mod} + \frac{m_1+m_2}{m_0+m_1+m_2} P_{index} \quad (22)$$

1) *Bit error rate for index bits (*$\mathrm{P_{index}}$): An error will occur if the magnitude of the decision variable for the idle subcarrier, denoted as $\left|W_{r,\delta_f,\delta_t}\right|$, is higher than the minimum magnitude of the decision variable of the busy subcarriers, denoted as $\left|W_{r,i,j}\right|$, where $1 < i \leq N_f, 1 < j \leq N_t$. The formula for evaluating the symbol error rate (SER) of index bits $P_{SER-index}$ is as follows [21],[24],[25], [28]:

$$P_{SER-index} = Pr\left[\left|W_{r,\delta_f,\delta_t}\right| > min\left(\left|W_{r,i,j}\right|\right)\right] = \int_0^{+\infty} \left(1 - \left(1 - F_{|W_{r,i,j}|}(y,\mu_2,\sigma_2^2)\right)^{N_f N_t - 1}\right) f_{\left|W_{r,\delta_f,\delta_t}\right|}(y,\mu_1,\sigma_1^2)dy \quad (23)$$

The probability density function (PDF) is represented by $f_{\left|W_{r,\delta_f,\delta_t}\right|}$, while the cumulative distribution function (CDF) is represented by $F_{|W_{r,i,j}|}$. Both of these functions follow the folded normal distribution and may be mathematically represented as [21], [24]:

$$F_{|W_{r,i,j}|}(y,\mu_2,\sigma_2^2) = \frac{1}{2}\left[erf\left(\frac{y-\mu_2}{\sqrt{2\sigma_2^2}}\right) + erf\left(\frac{y+\mu_2}{\sqrt{2\sigma_2^2}}\right)\right] \quad (24)$$

$$f_{\left|W_{r,\delta_f,\delta_t}\right|}(y,\mu_1,\sigma_1^2) = \frac{1}{\sqrt{2\pi\sigma_1^2}}\left(e^{-\frac{(y-\mu_1)^2}{2\sigma_1^2}}\right) \quad (25)$$

By substituting Eqs. (20), (21), (24), and (25) into Eq. (23), the expression for $P_{SER-index}$ may be written as follows:

$$P_{SER-index} = \frac{1}{\sqrt{0.5N_0^2\left[2\gamma_0\,\gamma_b + \frac{R}{N_t}\right]}} \times \int_0^{+\infty} \left(1 - \left(1 - 0.5\left[erf\left(\frac{y - N_0\,\gamma_0\,\gamma_b}{\sqrt{0.5N_0^2\left(2\gamma_0\,\gamma_b + \frac{2\gamma_0\,\gamma_b}{N_t} + \frac{R}{N_t}\right)}}\right) + erf\left(\frac{y + N_0\,\gamma_0\,\gamma_b}{\sqrt{0.5N_0^2\left(2\gamma_0\,\gamma_b + \frac{2\gamma_0\,\gamma_b}{N_t} + \frac{R}{N_t}\right)}}\right)\right]\right) \quad (26)$$

depends on $P_{SER-index}$; P_{index} may be obtained as follows [25]:

$$P_{index} = \frac{2^{(m_0+m_1+m_2)}}{2^{m_1}\,2^{m_2}-1} P_{SER-index} \quad (27)$$

2) *Bit error rate for modulated bits (*P_{mod}*)*: Two statuses indicate the presence of the modulated bit mistake. The first situation arises when the subcarrier-time index bits are accurately retrieved, but an error is present in the modulated bits. Hence, BER of the modulated bits P_{DCSK} in this particular condition is calculated as:

$$P_{DCSK} = \frac{1}{2} erfc\left[\left(\frac{2\sigma_1^2}{\mu_1^2}\right)^{-\frac{1}{2}}\right]$$

$$= \frac{1}{2} erfc \left[\left(\frac{(Gm_0+N_t)(1+N_t)}{GN_t(m_0+m_1+m_2)\gamma_b} + \frac{R}{2N_t} \frac{(Gm_0+N_t)^2}{G^2(m_0+m_1+m_2)^2(\gamma_b)^2} \right)^{-\frac{1}{2}} \right] \quad (28)$$

In the second situation, if an error occurs in the subcarrier-time index bits, resulting in a recovery of modulated bits from the incorrect correlator. Consequently, the probability of accurate detection may be expressed as (0.5). Based on these two statuses, P_{mod} is denoted by:

$$P_{mod} = P_{DCSK}(1 - P_{SER-index}) + 0.5 P_{SER-index} \quad (29)$$

By substituting Eqs. (27) and (29) into Eq. (22), we may determine the conditional probability P_{BER}.

Averaging the BER in (22) over γ_b yields the overall BER equation of the suggested system through multipath Rayleigh fading channel, defining $\overline{\gamma_b} = \frac{E_b \sum_l^P E(\alpha_{r,l}^2)}{N_0}$ [21], [24]:

$$P_{Rayleigh} = \int_0^{+\infty} P_{BER} \; f(\gamma_b) \; d\gamma_b \quad (30)$$

$$f(\gamma_b) = \frac{(\gamma_b)^{G-1}}{(G-1)!\,(\overline{\gamma_b})^G} \exp\left(-\frac{\gamma_b}{\overline{\gamma_b}}\right) \quad (31)$$

This equation is also valid for the AWGN scenario, where just the first path having a propagation gain α_l=1 and chip delay τ_l=0 is taken into account.

5. Numerical result and discussion

This section evaluates the theoretical and simulated BER performance of the suggested GFTIM-DCSK-II system through both the AGWN and multipath Rayleigh fading channels. The parameters of a multipath Rayleigh fading channel are set as follows: path delays τ_1 = 0, τ_2 = 2, and τ_3 = 5, the fading path P = 3, with equal average power gains E [α_1] = E [α_2] = E [α_3] = $\frac{1}{3}$.

5.1 Performance evaluation

The parameters for simulating the GFTIM-DCSK-II system are established as follows: the system employs 257 subcarriers, the frequency index, and time index are represented by the values q=8, m_1=1,2,3, and m_2=1,2,3, respectively; and the parameter β=400. Figs. 6 and 7 display the theoretical and simulated BER performance of the

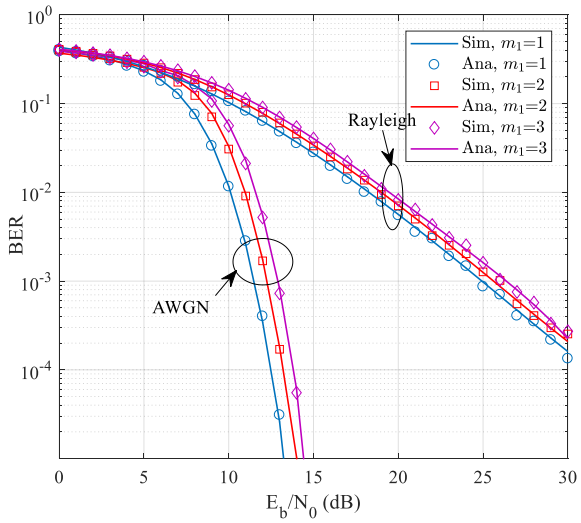

Figure. 6 BER against E_b/N_0 for GFTIM-DCSK-II system in AWGN and multipath Rayleigh fading channels, where β=400, q=8, m_2=2, and m_1=1,2,3

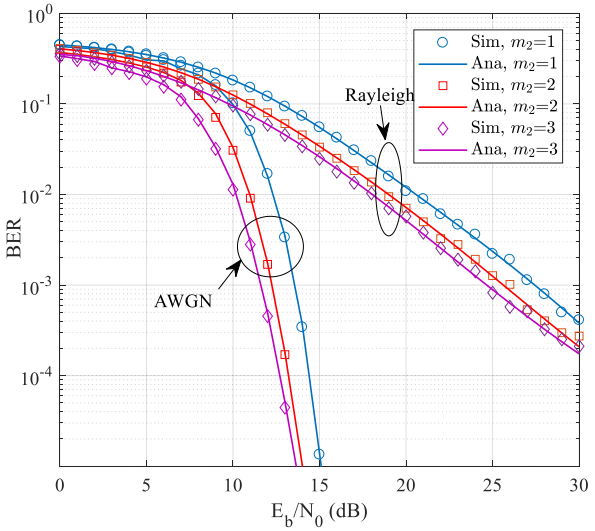

Figure. 7 BER against E_b/N_0 for GFTIM-DCSK-II system in AWGN and multipath Rayleigh fading channels, where β=400, q=8, m_1=2, and m_2=1,2,3

jjsuggested GFTIM-DCSK-II system under several channel conditions, including AWGN and multipath Rayleigh fading channels. Additionally, it illustrates the impact of parameters m_1 and m_2 on the BER performance of the GFTIM-DCSK-II system. As can be seen, our theoretical analysis of the results of simulations is verified by their excellent agreement with the theoretical BER expressions. Fig. 6 shows, that when m_2 and spreading factor R is held constant, increasing m_1 in the proposed system leads to a deterioration in the BER performance.

In Fig. 7, as m_2 rises, the BER performance of the GFTIM-DCSK-II system. As can be seen, our

theoretical analysis of the results of simulations is verified by their system enhancement while m_1 and β are constant. For instance, in an AWGN channel with constant m_1 and β, the GFTIM-DCSK-II system with m_2= 3 achieves a gain of 1.25 dB at a BER of 10^{-4} compared to that with m_2 = 2.

5.2 Performance comparison with other schemes

Fig. 8 illustrates the comparison of the BER performance between the suggested GFTIM-DCSK-II system and the CI-DCSK2 system. In this comparison, the data rate and spread factor are set as follows: $\varepsilon = 76/\beta Tc$, $\varepsilon = 144/\beta Tc$, and $\beta = 400$, respectively. The GFTIM-DCSK-II system performance of BER is superior to the CI-DCSK2 system through multipath Rayleigh fading and AWGN channels, as illustrated in this Figure. For example, the GFTIM-DCSK-II system outperforms the CI-DCSK2 system by about 5 dB across the AWGN channel at a BER of 10^{-4} when $\varepsilon = 76/\beta Tc$, $69/\beta Tc$ for GFTIM-DCSKII and CI-DCSK2, respectively. Furthermore, there is a slight improvement in the GFTIM-DCSK-II system's performance while a slight decline in the CI-DCSK2 system's performance as ε increases. On the multipath Rayleigh fading channel, similar conclusions may also be made from the results.

Fig. 9 presents a comparison between the Bit Error Rate (BER) performance of the GFTIM-DCSK-II system and the GSIM-DCSKII system at $\varepsilon = 144/\beta Tc$, $\varepsilon = 288/\beta Tc$ and $\beta = 600$. According to this Figure, the GFTIM-DCSKII system outperforms the GSIM-DCSKII system in terms of BER performance over both multipath

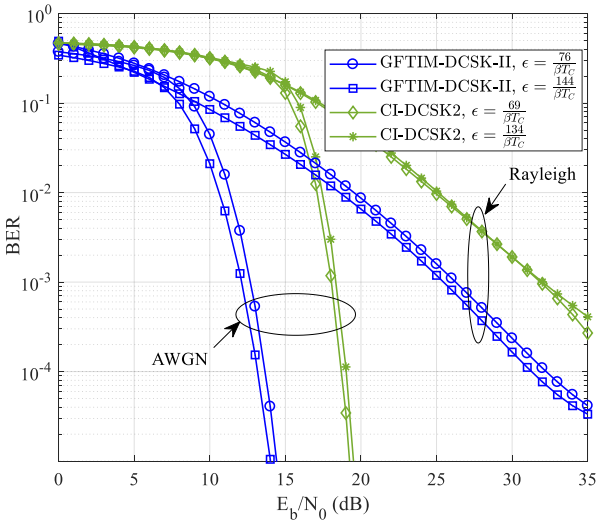

Figure. 8 BER performance comparisons of GFTIM-DCSK-II and CI-DCSK2 over AWGN and multipath Rayleigh fading channels, where $\beta = 400$, and q=8

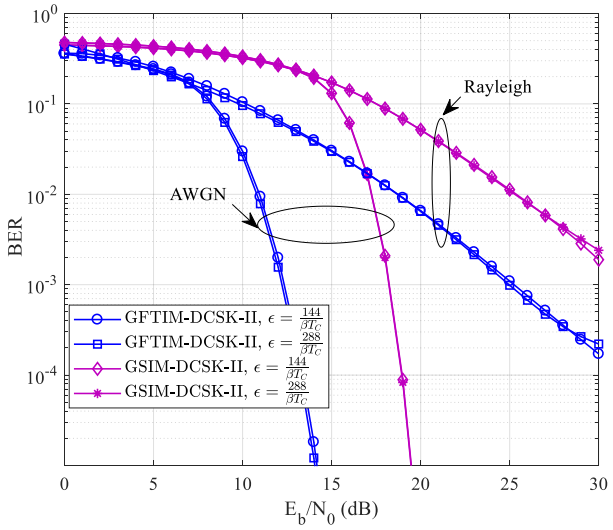

Figure. 9 BER performance comparisons of GFTIM-DCSK-II and GSIM-DCSKII over AWGN and multipath Rayleigh fading channels, where $\beta = 600$, and q=8

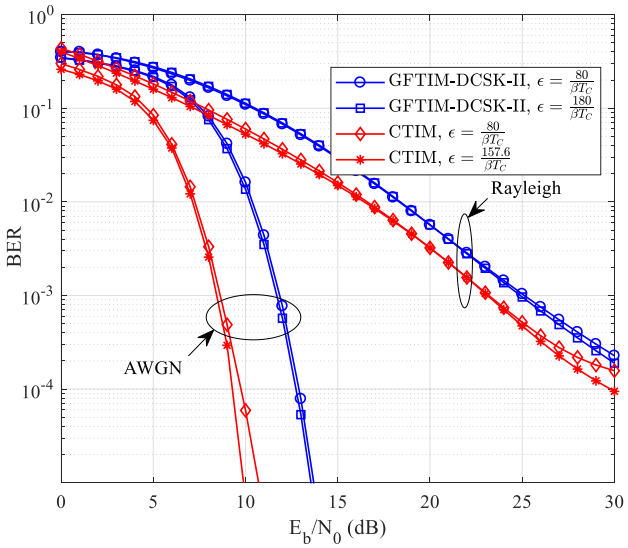

Figure. 10 BER performance comparisons of GFTIM-DCSK-II and CTIM-DCSK over AWGN and multipath Rayleigh fading channels at the same data rate, where q=8, and $\beta = 400$

Rayleigh fading and AWGN channels. for instance, the GFTIM-DCSK-II system achieves a gain of around 5.5 dB in comparison with the GSIM-DCSKII system with a BER of 10^{-4} across AWGN channel when $\varepsilon = 144/\beta Tc$ and around 6 dB with a BER of 10^{-2} across Rayleigh fading channel at the same data rate.

Figs. 10 and 11 illustrate the BER performance comparison between GFTIM-DCSK-II and CTIM-DCSK within both the AWGN channel and the multipath Rayleigh fading channel with $\beta = 400$. In Fig. 10, for the same data rate $\varepsilon = 80/\beta Tc$ and

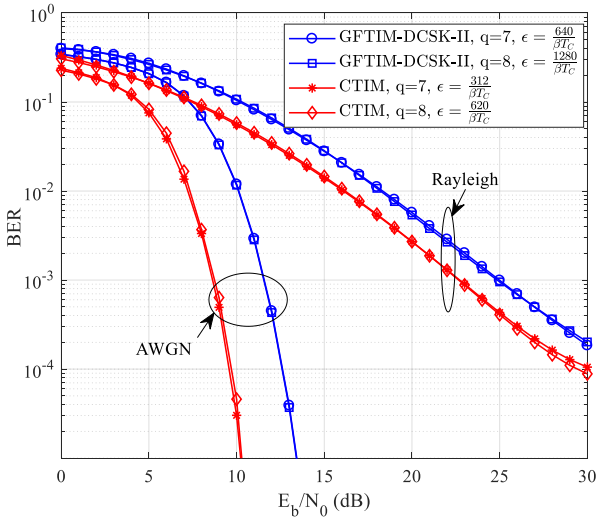

Figure. 11 BER performance comparisons of GFTIM-DCSK-II and CTIM-DCSK over AWGN and multipath Rayleigh fading channels with different values of q at $\beta = 400$

$\varepsilon = 180/\beta Tc$ GFTIM-DCSK-II exhibits a degradation in BER performance compared to CTIM-DCSK at a constant number of subcarriers q. Fig. 11 shows this comparison for the same number of subcarriers q=7,8. From Fig. 11 GFTIM-DCSK-II may be regarded as a scheme that offers a larger data rate compared to CTIM-DCSK but at the cost of a decrease in BER performance over both the AWGN and multipath Rayleigh fading channels.

6. Conclusion

This study presents the combination of DCSK with grouping frequency-time index modulation (GFTIM) to create a novel chaos-based modulation technique with enhanced system performance. This system uses the concept of GFTIM-DCSK-II to send additional bits of information by employing a novel combination of frequency and time dimensions to map the information bits. As additional information is transmitted with the frequency and time indices, the suggested system's data throughput, spectrum efficiency, and energy efficiency increase significantly.

When comparing the proposed system with existing DCSK schemes in different situations it shows improvement in energy efficiency, it saves around 40% more energy than CTIM-DCSK with q /m_1/m_2= 8/1/1 but 10% less than GSIM-DCSKII and the enhancement in energy is done with an increase in m_2 and decrease in m_1, also the proposed system show enhancement in the spectral efficiency around five times more than CTIM-DCSK and GSIMDCSK-II with q /m_1/m_2= 8/1/4 and this value is increased as an increase in m_2. Furthermore, the comparison of the proposed system with other DCSK schemes makes it evident that the suggested system has less complexity.

After deriving the theoretical BER expression of the suggested system across AWGN and multipath Rayleigh fading channels, the simulation results confirm that our derivation is accurate. When comparing the proposed system with existing DCSK schemes in different situations, it is evident that the suggested system is superior to them in terms of BER performance, it was enhanced by around 5 dB than CI-DCSK2 and GSTIM-DCSKII across the AWGN channel at a BER of 10^{-4} at the same data rate. On the multipath Rayleigh fading channel, the BER is enhanced around 5 dB at 10^{-3} and 6 dB at 10^{-2} for the same data rate compared with CI-DCSK2 and GSIM-DCSK2, respectively.

The suggested modulation technique largely satisfies the requirements of 5G wireless systems by significantly enhancing data throughput, minimizing power consumption, operating with low latency and power profile, and demonstrating promising overall performance.

Notation list:

Symbol	Description
m_1,m_2	Number of Frequency and time indices bits
m_0	Number Modulated bits
m	Number of total bits for each sub-block
N_f	Number of subcarriers for each sub-block
N_t	Number of time slots for each sub-block
δ_f,δ_t	Frequency and time indices symbols for each sub-block
G	Number of sub-blocks
R	Duration of a reference-chaotic signal
r	Symbol duration
β	Spreading factor of the GFTIM-DCSK-II system
M	Total number of subcarriers
μ_1,μ_2	The means of $W_{r,i,j}$
σ_1^2,σ_2^2	The variances of $W_{r,i,j}$
γ_b, $\overline{\gamma_b}$	The bit-to-noise ratio and its average
$d_{(i,j)}^{g}$	The information sequence in each sub-block
ε	The data rate

Conflicts of Interest

The authors declare no conflict of interest.

Author Contributions

The first author performed conceptualization, methodology, software, formal analysis, resources, data curation, and writing—original draft preparation. The second author assumed the role of supervision, performed a comprehensive work review, and conducted the process of validation.

References

[1] C. Tse and F. Lau, *Chaos-based digital communication systems*, Heidelberg, Germany: Springer-Verlag, 2003.

[2] H. Dedieu, M. P. Kennedy, and M. Hasler, "Chaos shift keying: modulation and demodulation of a chaotic carrier using self-synchronizing Chua's circuits", *IEEE Transactions on Circuits and Systems II: Analog and Digital Signal Processing*, Vol. 40, No. 10, pp. 634-642, 1993.

[3] N. Al Bassam and O. Al-Jerew, "Design of Enhanced Permutation Differential Chaos Shift System Using Signal Reference with Dual Modulation", *IEEE Access*, Vol. 9, pp. 111915-111924, 2021.

[4] G. Kaddoum, "Wireless chaos-based communication systems: A comprehensive survey", *IEEE Access*, Vol. 4, pp. 2621-2648, 2016.

[5] Z. Galias and G. M. Maggio, "Quadrature chaos-shift keying: Theory and performance analysis", *IEEE Transactions on Circuits and Systems I: Fundamental Theory and Applications*, Vol. 48, No. 12, pp. 1510-1519, 2001.

[6] H. Yang and G. Jiang, "High-efficiency differential-chaos-shift-keying scheme for chaos-based noncoherent communication", *IEEE Transactions on Circuits and Systems II: Express Briefs*, Vol. 59, No. 5, pp. 312-316, 2012.

[7] G. Kaddoum and E. Soujeri, "NR-DCSK: A noise reduction differential chaos shift keying system", *IEEE Transactions on Circuits and Systems II: Express Briefs*, Vol. 63, No. 7, pp. 648-652, 2016.

[8] G. Kaddoum, E. Soujeri, and Y. Nijsure, "Design of a short reference noncoherent chaos-based communication systems", *IEEE Transactions on Communications*, Vol. 64, No. 2, pp. 680-689, 2016.

[9] G. Kaddoum, E. Soujeri, C. Arcila, and K. Eshteiwi, "I-DCSK: An improved noncoherent communication system architecture", *IEEE Transactions on Circuits and Systems II: Express Briefs*, Vol. 62, No. 9, pp. 901-905, 2015.

[10] H. Yang, W. K. Tang, G. Chen, and G. Jiang, "Multi-carrier chaos shift keying: System design and performance analysis", *IEEE Transactions on Circuits and Systems I: Regular Papers*, Vol. 64, No. 8, pp. 2182-2194, 2017.

[11] M. Agiwal, A. Roy, and N. Saxena, "Next generation 5G wireless networks: A comprehensive survey", *IEEE Communications Surveys & Tutorials*, Vol. 18, No. 3, pp. 1617-1655, 2016.

[12] E. Basar, M. Wen, R. Mesleh, M. Di Renzo, Y. Xiao, and H. Haas, "Index modulation techniques for next-generation wireless networks", *IEEE Access*, Vol. 5, pp. 16693-16746, 2017.

[13] T. Mao, Q. Wang, Z. Wang, and S. Chen, "Novel index modulation techniques: A survey", *IEEE Communications Surveys & Tutorials*, Vol. 21, No. 1, pp. 315-348, 2018.

[14] E. Soujeri, G. Kaddoum, M. Au, and M. Herceg, "Frequency index modulation for low complexity low energy communication networks", *IEEE Access*, Vol. 5, pp. 23276-23287, 2017.

[15] W. Xu, T. Huang, and L. Wang, "Code-shifted differential chaos shift keying with code index modulation for high data rate transmission", *IEEE Transactions on Communications*, Vol. 65, No. 10, pp. 4285-4294, 2017.

[16] X. Cai, W. Xu, D. Wang, S. Hong, and L. Wang, "An M-ary orthogonal multilevel differential chaos shift keying system with code index modulation", *IEEE Transactions on Communications*, Vol. 67, No. 7, pp. 4835-4847, 2019.

[17] M. Herceg, D. Vranješ, G. Kaddoum, and E. Soujeri, "Commutation code index DCSK modulation technique for high-data-rate communication systems", *IEEE Transactions on Circuits and Systems II: Express Briefs*, Vol. 65, No. 12, pp. 1954-1958, 2018.

[18] G. Kaddoum, M. F. Ahmed, and Y. Nijsure, "Code index modulation: A high data rate and energy efficient communication system", *IEEE Communications Letters*, Vol. 19, No. 2, pp. 175-178, 2014.

[19] G. Kaddoum, Y. Nijsure, and H. Tran, "Generalized code index modulation technique for high-data-rate communication systems", *IEEE Transactions on Vehicular Technology*, Vol. 65, No. 9, pp. 7000-7009, 2015.

[20] G. Kaddoum, F. Richardson, and F. Gagnon, "Design and analysis of a multi-carrier

differential chaos shift keying communication system", *IEEE Transactions on Communications*, Vol. 61, No. 8, pp. 3281-3291, 2013.

[21] G. Cheng, L. Wang, W. Xu, and G. Chen, "Carrier index differential chaos shift keying modulation", *IEEE Transactions on Circuits and Systems II: Express Briefs*, Vol. 64, No. 8, pp. 907-911, 2016.

[22] G. Cheng, X. Chen, W. Liu, and W. Xiao, "GCI-DCSK: Generalized carrier index differential chaos shift keying modulation", *IEEE Communications Letters*, Vol. 23, No. 11, pp. 2012-2016, 2019.

[23] G. Cheng, L. Wang, Q. Chen, and G. Chen, "Design and performance analysis of generalised carrier index M-ary differential chaos shift keying modulation", *IET Communications*, Vol. 12, No. 11, pp. 1324-1331, 2018.

[24] W. Dai, H. Yang, Y. Song, and G. Jiang, "Two-layer carrier index modulation scheme based on differential chaos shift keying", *IEEE Access*, Vol. 6, pp. 56433-56444, 2018.

[25] X. Cai, W. Xu, L. Wang, and F. Xu, "Design and performance analysis of differential chaos shift keying system with dual-index modulation", *IEEE Access*, Vol. 7, pp. 26867-26880, 2019.

[26] M. Au, G. Kaddoum, F. Gagnon, and E. Soujeri, "A joint code-frequency index modulation for low-complexity, high spectral and energy efficiency communications", *arXiv preprint arXiv:1712.07951*, 2017.

[27] Y. Fang, J. Zhuo, H. Ma, S. Mumtaz, and Y. Li, "Design and analysis of a new index-modulation-aided DCSK system with frequency-and-time resources", *IEEE Transactions on Vehicular Technology*, Vol. 72, No. 6, pp. 7411-7425, 2023.

[28] F. S. Hasan, "Design and analysis of grouping subcarrier index modulation for differential chaos shift keying communication system", *Physical Communication*, Vol. 47, pp. 101325, 2021.

[29] B. Nazar and F. S. Hasan, "Joint Grouping Subcarrier and Permutation Index Modulations Based Differential Chaos Shift Keying System", *Physical Communication*, Vol. 61, pp. 102213, 2023.

[30] F. S. Hasan and A. A. Valenzuela, "Design and analysis of an OFDM-based orthogonal chaotic vector shift keying communication system", *IEEE Access*, Vol. 6, pp. 46322-46333, 2018.